Supporting Information

Mechanism study on organic ternary photovoltaics with 18.3% certified efficiency: from molecule to device

Yaokai Li,[a][‡] Yuan Guo,[b][‡] Zeng Chen,[c][‡]Lingling Zhan,[a][‡] Chengliang He,[a] Zhaozhao Bi,[d] Nannan Yao,[e] Shuixing Li,[a] Guanqing Zhou,[c] Yuanping Yi, *[f] Yang (Michael) Yang,[g] Haiming Zhu,[c] Wei Ma,[d] Feng Gao,[e] Fengling Zhang,[e] Lijian Zuo,*[a,h] Hongzheng Chen*[a]

[a]State Key Laboratory of Silicon Materials, MOE Key Laboratory of Macromolecular Synthesis and Functionalization, Department of Polymer Science and Engineering, Zhejiang University, Hangzhou 310027, P. R. China

[b]School of Light Industry and Engineering, Qilu University of Technology (Shandong Academy of Sciences), Jinan 250353, P. R. China

[c]Department of Chemistry, Zhejiang University, Hangzhou 310027, P. R. China

[d]State Key Laboratory for Mechanical Behavior of Materials, Xi'an Jiaotong University, Xi'an 710049, P. R. China

[e]Department of Physics, Chemistry and Biology (IFM), Linköping University, Linköping, SE-58183, Sweden

[f]Beijing National Laboratory for Molecular Sciences, CAS Key Laboratory of Organic Solids, Institute of Chemistry, Chinese Academy of Sciences, Beijing 100190, P. R. China

[g]State Key Laboratory of Modern Optical Instrumentation, Institute for Advanced Photonics, College of Optical Science and Engineering, Zhejiang University, Hangzhou 310027, P. R. China

[h]Zhejiang University-Hangzhou Global Scientific and Technological Innovation Center, Hangzhou 310014, P. R. China

‡Contributed equally to this work.

*Corresponding authors: zjuzlj@zju.edu.cn, ypyi@iccas.ac.cn, hzchen@zju.edu.cn

Experimental sections

Materials: All reagents and solvents were used directly as received, unless otherwise specified. PBDB-TF, PFN-Br, IT-4F and BTP-eC9 were purchased from Solarmer Materials Inc. PEDOT:PSS (Clevios P VP 4083) was purchased from Heraeus Inc., Germany. BTP-S2 was synthesized in our lab as reported.[1]

Device fabrications: Organic solar cells were fabricated on ITO glass substrates with the conventional structure of ITO/PEDOT:PSS/Active layer/PFN-Br /Ag. The ITO glass substrates were cleaned by sonication using detergent, deionized water, acetone and isopropanol consecutively for 15 min in each step before fabrication. The precleaned ITO substrates were treated in an ultraviolet ozone generator for 10 min, followed by deposition of PEDOT:PSS (Baytron PAI 4083). After baking the PEDOT:PSS layer in air at 150 °C for 10 min, the substrates were transferred to a glovebox. The active layer was spin coated from 17.6 mg/ml solution dissolved in chloroform (D:A = 1:1.2, 0.25% v/v DIO) at 2200 rpm or so for 30 s to form an active layer. Then the devices were annealed at 100 °C for 10 min. Later, when the film cooled to room temperature, a layer of PFN-Br (0.5 mg/ml in methanol) was deposited by spin coating at 3500 rpm for 20 s. Then the silver electrode was deposited by thermal evaporation under a base pressure of 1×10^{-4} Pa at the speed of 2 Å/s. The active cell area of our device is 0.06 cm^2, and the aperture for measurement is 0.0473 cm^2, which is certified by National Institue of Metrology (NIM) and Fujian Metrology Institute.

Solar cell characterization: The J-V measurement was performed via the solar simulator (SS-F5-3A, Enlitech) along with AM 1.5G spectrum, whose intensity was calibrated by a standard silicon solar cell (SRC-2020, Enlitech) with KG-2 filter at 100 mW/cm^2. The scan direction is from -0.2 V to 1.2 V, with a scan step of 0.01 V and the delay time of 1 ms. The external quantum efficiency (EQE) data were obtained from the solar-cell spectral-response

measurement system (QE-R, Enlitech). The best device has been sent for certification at third-authorized party at National PV Industry Measurement and Testing Center.

CV characterization: Cyclic voltammetry (CV) was done on a CHI600A electrochemical workstation with Pt disk, Pt plate, and standard calomel electrode (SCE) as working electrode, counter electrode, and reference electrode, respectively, in a 0.1 mol/L tetrabutylammoniumhexafluorophosphate (Bu_4NPF_6) acetonitrile solution. The CV curves were recorded versus the potential of SCE, which was calibrated by the ferrocene-ferrocenium (Fc/Fc_+) redox couple (4.8 eV below the vacuum level). The equation of $E_{LUMO/HOMO} = -e(E_{red/ox}+4.41)$ (eV) was used to calculate the LUMO and HOMO levels (the redox potential of Fc/Fc_+ is found to be 0.39 V).

AFM characterization: Topographic images of the films were measured from a VeecoMultiMode AFM in tapping mode, and the scanning rate for a 1μm $\times$ 1μm image was 1.0 Hz.

Absorption characterization. Absorption spectra were measured with a U-4100 (HITACHI) UV-vis spectrophotometer.

GIWAXS Measurements. GIWAXS measurements were performed at beamline 7.3.3 at the Advanced Light Source. Samples were prepared on Si substrates using identical blend solutions as those used in devices. The 10 keV X-ray beam was incident at a grazing angle of 0.12°-0.16°, selected to maximize the scattering intensity from the samples. The scattered X-rays were detected using a Dectris Pilatus 2M photon counting detector.

FTPS-EQE Measurements. FTPS-EQE was measured using Vertex 70 from Bruker Optics, equipped with a quartz tungsten halogen lamp, quartz beam splitter and external detector option.

A low-noise current amplifier (SR570) was used to amplify the photocurrent produced on illumination of the photovoltaic devices with light modulated by the Fourier transform infrared spectroscope (FTIR). The output voltage of the current amplifier was fed back into the external detector port of the FTIR, to be able to use the FTIR's software to collect the photo current spectrum.

EL Measurements. EL spectra were measured using a light guide positioned close to the sample. The bias was applied on the devices using a Keithley 2400 Source Meter. The detector was a Newton EM-CCD Si array detector at -60 °C with a Shamrock SR-303i spectrography from Andor Tech.

EQE$_{EL}$ Measurements. EQE$_{EL}$ values were obtained from an in-house-built system including a Hamamatsu silicon photodiode 1010B, a Keithley 2400 Source Meter to provide voltage and record injected current, and a Keithley 485 Picoammeter to measure the emitted light intensity.

Space-Charge-Limited current (SCLC) measurement: The charge carrier mobilities of the binary and ternary devices were measured using the SCLC method. Hole-only devices were fabricated in a structure of ITO/PEDOT:PSS/Active Layer/MoO$_3$/Ag. Electron-only devices were fabricated in a structure of ITO/ZnO/Active Layer/PFN-Br/Ag. The device characteristics were extracted by modeling the dark current under forward bias using the SCLC expression described by the Mott-Gurney law:

$$J = \frac{9}{8} \varepsilon_r \varepsilon_0 \mu \frac{V^2}{L^3}$$

Here, $\varepsilon_r \approx 3$ is the average dielectric constant of the blend film and ε_0 is the permittivity of the free space, μ is the carrier mobility, L is the thickness of the film, and V is the applied voltage.

Molecular Dynamics Simulations. The atomistic MD simulations were performed with the Gromacs-4.6.7 software package based on the general AMBER force field with the RESP charges.[2-4] As the same as the previous work for Y6, the torsion potentials between the central backbone and the terminal acceptor groups for BTP-eC9 and BTP-S2 were reparametrized according to DFT calculations.[5] The pristine BTP-eC9, BTP-S2 thin-films and the mixed thin-film (BTP-eC9:25wt%BTP-S2) were built and imitated using the following procedure: (1) Randomly placing total 400 molecules in a $25 \times 25 \times 25$ nm^3 box to generate an initial geometry; (2) 5 ns of simulation at 800 K and 100 bar to make molecules close together quickly; (3) 10 ns of simulation at 800 K and 1 bar, then cooling down to 300 K in 5 ns; (4) 10 ns of equilibration at 300 K and 1 bar (equilibration). The velocity rescaling thermostat and the Berendsen barostat under the NPT ensemble were applied to control the temperature and pressure, respectively.[6, 7] But for the final 10 ns of equilibration, the Nosé–Hoover thermostat and the Parrinello–Rahman barostat were used to obtain better equilibrium conformations.[8-10]

Transient absorption spectroscopy. For femtosecond transient absorption spectroscopy, the fundamental output from Yb:KGW laser (1030 nm, 220 fs Gaussian fit, 100 kHz, Light Conversion Ltd) was separated to two light beams. One was introduced to NOPA (ORPHEUS-N, Light Conversion Ltd) to produce a certain wavelength as the pump beam (here we use 550 nm, 750 nm and 925 nm, , 30 fs pulse duration), the other was focused onto a YAG plate to generate white light continuum as the probe beam. The pump and probe beams overlapped on the sample at a small angle less than 10°. The transmitted probe light from sample was collected by a linear CCD array . The transmitted probe light with (Tpump) and without (Tunpump) pump were collected and the normalized transmittance change $\Delta T/T$ was calculated by $\Delta T/T = (T_{pump} - T_{unpump})/T_{unpump}$. The samples were loaded in a cryostat for temperature dependent measurement. Noted that since all the samples were measured at N_2 atmosphere, limited by the measurement factors, the real excitation power will be smaller.

Steady state PL Steady-state PL were detected using a home-setup microfluorescence system. The excitation light (515nm) was generated by a CW laser. PL spectra were measured using a spectrograph (Princeton Instruments) with a liquid-N_2-cooled CCD.

Supplementary Figures.
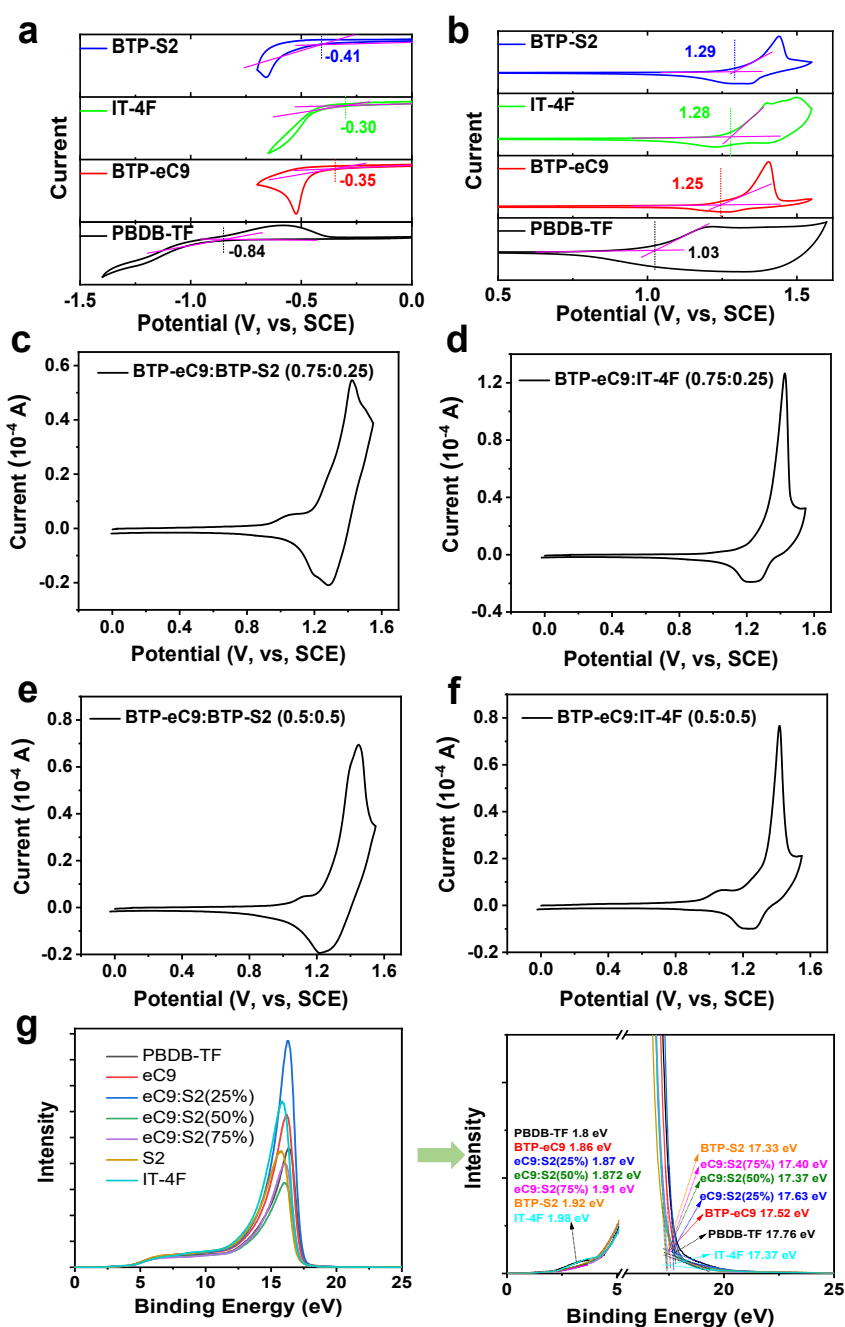
Figure S1. a), b) Cyclic voltammograms of PBDB-TF,BTP-eC9, IT-4F, BTP-S2 and Fc/Fc+. The HOMO and LUMO positions are determined by the point of intersection using two tangent lines at the onsets of oxidation or reduction waves. The equation of $E_{LUMO/HOMO} = -e(E_{red/ox}+4.41)$ (eV) was used to calculate the LUMO and HOMO levels Cyclic voltammograms of mixed acceptors; c) BTP-eC9:BTP-S2 (0.75:0.25); d) BTP-eC9:IT-4F (0.75:0.25), e) BTP-eC9:BTP-S2 (0.5:0.5); f) BTP-eC9:IT-4F (0.5:0.5). g) UPS spectra of different blend systems.
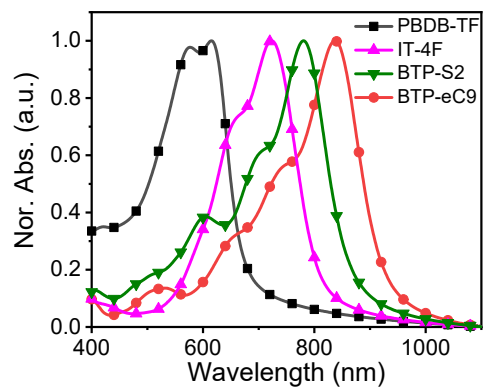
Figure S2. Normalized UV-vis absorption spectra of PBDB-TF, IT-4F, BTP-eC9, and BTP-S2.

检 测 报 告
Test Report

报告编号：21Q3-00024
Report No.

客 户 名 称 Name of Customer	Department of Polymer Science & Engineering, Zhejiang University
联 络 信 息 Contact Information	Zhejiang University, 38 Zheda Road, Hangzhou, Zhejiang Province, 310027, P. R. China
物 品 名 称 Name of Items	Organic Solar Cells
型 号／规 格 Type /Specification	1.5cm×1.5cm
物 品 编 号 Items No	PM6:C9:S2
制 造 厂 商 Manufacturer	Department of Polymer Science & Engineering, Zhejiang University
物品接收日期 Items Receipt Date	2021-01-28
检 测 日 期 Test Date	2021-01-29

（盖章处）
Stamp

批 准 人　　　　罗海燕
Approved by
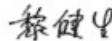
核 验 员　　　　黎健生
Checked by
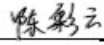
检 测 员　　　　陈彩云
Test by

发布日期　2021　年　02　月　04　日
Date of Report　　Year　　month　　Day

扫一扫 查真伪

报告编号：21Q3-00024
Report No.

1. 检测机构说明：
Testing institutions that

本院为国家法定计量检定机构，国家光伏产业计量测试中心依托本院检测技术开展检测。本院/本中心质量管理体系符合 GB/T 27025（ISO/IEC 17025，IDT）标准要求。
The institute is a national legal metrological institution, National PV Industry Measurement and Testing Center carrys out testing relying on the institute's testing technology. The Center's quality management system meets the requirements of GB/T 27025（ISO/IEC 17025, IDT) standard.

2. 本次检测所依据的检测方法（代号及名称）：
Reference documents from the test (code/name)

IEC 60904-1-2020 光伏器件-第一部分：光伏电流-电压特性的测量；IEC 60904-8:2014 光伏器件-第 8 部分光伏器件的光谱响应度测量

3. 本次检测所使用的主要测量仪器：
Measurement standards used in this test

仪器名称 Name	仪器编号 Number	测量范围 Measuring Range	不确定度/或准确度等级/或最大允许误差 Uncertainty or Accuracy Class or Maximum Permissible Error	溯源机构名称/证书编号 Name of traceability institution/Certificate No.	有效期限 Due date
系统源表（电子负载）	4082810	100 nA~3 A;(0.1~40) V	U_{rel}=0.005% (k=2)	上海市计量院 2020F11-10-2336101001	2021-02-27
WPVS 单晶硅标准电池	015-2014	(300~1200) nm	U_{rel}=1.3% (k=2)	中国计量院 GXtc2019-0450	2021-03-05
Si 光电探测器	Si-2	(200~1100)nm	U=0.0027 A/W (k=2)	PTB73331 19 PTB	2021-05-13
自动影像测量仪	11656	X 轴：(0~195) mm；Y 轴：(0~195) mm	U=2 μm (k=2)	福建计量院 (MLY)A2/20-008990	2021-07-22
太阳模拟器	2015-006	(400~1100) nm;(800~1200) W/m²	光谱匹配度(400~1100) nm：U_{rel}=8.0% (k=2)；辐照度比（辐照度不均匀度、辐照度时间不稳定度）：U_{rel}=1.2% (k=2)	福建计量院 (MLY)Q2/20-000867	2021-06-30

4. 检测地点及环境条件：
Location and environmental condition for the test

地点：Room 108, Building 4, MinHou Scientific Research Base
Location

温度：25.3 ℃　　　相对湿度：45 %　　　其它：/
Temperature　　　　Relative Humidity　　　　　Others

5. 备注：/
Note

本报告提供的结果仅对本次被检的物品有效。
The data are valid only for the instrument(s) under testing.

检测报告续页专用
Continued page of test report

福建省计量科学研究院
FUJIAN METROLOGY INSTITUTE
（国家光伏产业计量测试中心）
National PV Industry Measurement and Testing Center

报告编号： 21Q3-00024
Report No.

检测结果/说明：
Results of Test and additional explanation.

1　Standard Test Condition (STC)： Total Irradiance：1000 W/m²

Temperature：25.0 ℃

Spectral Distribution：AM1.5G

2　Measurement Data under STC

Test Times	I_{sc} (mA)	V_{oc} (V)	I_{MPP} (mA)	V_{MPP} (V)	P_{MPP} (mW)	FF (%)	η (%)
1	1.256	0.8777	1.153	0.7513	0.8662	78.57	18.31
2	1.250	0.8781	1.150	0.7518	0.8646	78.77	18.28
3	1.253	0.8780	1.149	0.7511	0.8630	78.44	18.25
Average Value	1.253	0.8779	1.151	0.7514	0.8646	78.59	18.28

Mismatch factor: 1.002

3　I-V & P-V Characteristic Curves under STC
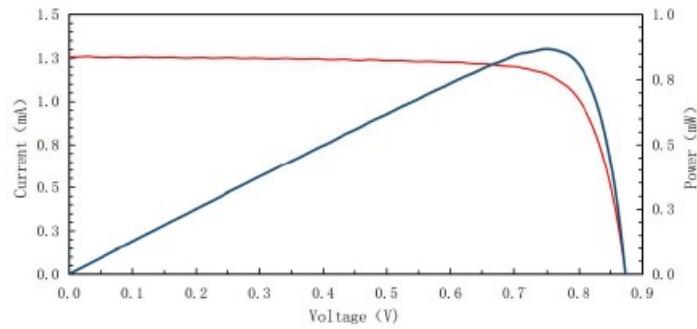
Figure 1. I-V and P-V characteristic curves of the measured sample under STC

福建省计量科学研究院
FUJIAN METROLOGY INSTITUTE
（国家光伏产业计量测试中心）
National PV Industry Measurement and Testing Center

报告编号：21Q3-00024
Report No.

检测结果/说明：
Results of Test and additional explanation.

4　Measurement Data of Relative Spectral Responsivity (SR) of the Measured Sample

Wavelength (nm)	SR(%)	Wavelength (nm)	SR(%)	Wavelength (nm)	SR(%)	Wavelength (nm)	SR(%)
300	0.38	530	65.53	760	94.08	990	0.45
310	1.98	540	67.89	770	95.00	1000	0.25
320	5.84	550	70.09	780	95.87	1010	0.29
330	11.23	560	71.61	790	97.17	1020	0.23
340	15.37	570	73.32	800	98.25	1030	0.28
350	17.71	580	74.48	810	98.96	1040	0.26
360	19.75	590	75.95	820	99.71	1050	0.27
370	21.44	600	77.46	830	100.00	1060	0.04
380	23.42	610	78.83	840	98.19	1070	0.03
390	27.11	620	79.98	850	95.13	1080	0.03
400	32.18	630	81.08	860	89.19	1090	0.03
410	37.35	640	82.03	870	80.62	1100	0.00
420	41.76	650	82.26	880	68.84	/	/
430	44.97	660	83.68	890	58.89	/	/
440	46.79	670	84.64	900	42.89	/	/
450	47.69	680	85.69	910	30.37	/	/
460	48.46	690	86.49	920	18.92	/	/
470	49.75	700	87.76	930	12.69	/	/
480	51.71	710	88.83	940	7.01	/	/
490	54.11	720	90.02	950	4.21	/	/
500	56.76	730	91.18	960	2.46	/	/
510	59.45	740	92.30	970	1.43	/	/
520	62.61	750	93.26	980	0.73	/	/

检测报告续页专用
Continued page of test report

福建省计量科学研究院
FUJIAN METROLOGY INSTITUTE
（国家光伏产业计量测试中心）
National PV Industry Measurement and Testing Center

报告编号： 21Q3–00024
Report No.

检测结果/说明：
Results of Test and additional explanation.

5   Relative Spectral Responsivity Curve
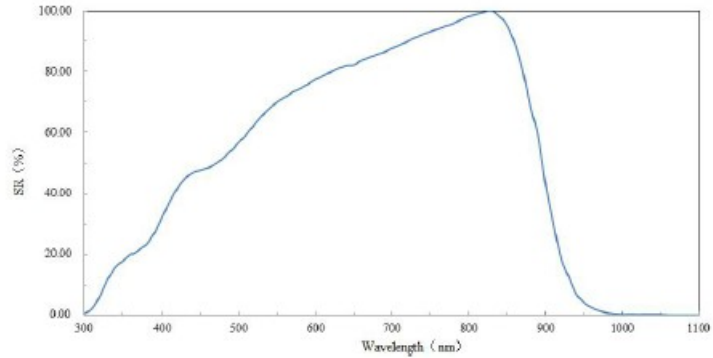
Figure 2. Relative spectral responsivity curve of the measured sample

6   Pictures of the Measured Sample

Figure 3. Obverse side of the measured sample

福建省计量科学研究院
FUJIAN METROLOGY INSTITUTE
（国家光伏产业计量测试中心）
National PV Industry Measurement and Testing Center

报告编号：21Q3-00024
Report No.

检测结果/说明：
Results of Test and additional explanation.

Figure 4. Reverse side of the measured sample
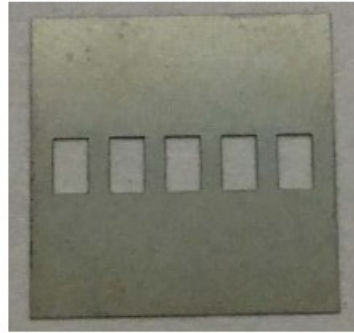
Figure 5. Mask used during test

Uncertainty of measurement results:

Short-Circuit Current: U_{rel}=2.5% (k=2); Open-Circuit Voltage: U_{rel}=1.0% (k=2);

Maximum Power: U_{rel}=2.2% (k=2); Efficiency: U_{rel}=2.2% (k=2); Fill Factor: U_{rel}=3.2% (k=2).

Relative Spectral Responsivity:

(300~400) nm: U_{rel} = 2.8% ~ 2.2% (k=2);

(400~1100) nm: U_{rel} = 2.2% ~ 2.6% (k=2).

说明：The effective area of the measured sample was 0.0473 cm^2.
Explanation

福建省计量科学研究院
FUJIAN METROLOGY INSTITUTE
（国家光伏产业计量测试中心）
National PV Industry Measurement and Testing Center

报告编号：21Q3-00024
Report No.

检测结果/说明：
Results of Test and additional explanation.

Reference documents from the test(code,name)
IEC 60904-1: 2020 Photovoltaic devices– Part 1: Measurement of photovoltaic current-voltage characteristics
IEC 60904-8: 2014 Photovoltaic devices– Part 8: Measurement of spectral responsivity of a photovoltaic (PV) device

Measurement standards used in this test					
Name	Number	Measuring Range	Uncertainty or Accuracy Class or Maximum Permissible Error	Name of traceability institution/Certificate No.	Due date
System SourceMeter （Electronic Load）	4082810	100 nA~3 A; (0.1~40) V	U_{rel}=0.005%(k=2)	Shanghai Institute of Metrology and Testing Technology / 2020F11-10-2336101001	2021-02-27
WPVS Monocrystalline Silicon Reference Cell	015-2014	(300~1200) nm	U_{rel}=1.3% (k=2)	National Institute of Metrology, China / GXtc2019-0450	2021-03-05
Si Photoelectric Detector	Si-2	(200~1100) nm	U=0.0027 A/W (k=2)	Physikalisch-Technische Bundesanstalt / 73331 19 PTB	2021-05-13
Automatic Image Measuring Instrument	11656	X-axis：(0~195) mm；Y-axis：(0~195) mm	U=2 μm (k=2)	Fujian Metrology Institute/ (MLY)A2/20-008990	2021-07-22
Solar Simulator	2015-006	(400~1100) nm；(800~1200) W/m²	Spectral Match(400~1100) nm： U_{rel}=8.0% (k=2)；Irradiance Ratio（Irradiance Nonuniformity、Irradiance Time Instability）：U_{rel}=1.2% (k=2)	Fujian Metrology Institute / (MLY)Q2/20-000867	2021-06-30

以下空白
Blank below

检测报告续页专用
Continued page of test report

Figure S3. Full version of certified report from Fujian Metrology Institute.
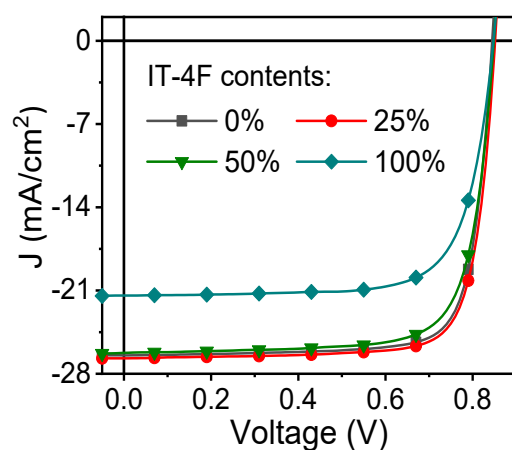
Figure S4. EQE spectra of PBDB-TF:BTP-eC9:IT-4F ternary OPVs with different IT-4F contents
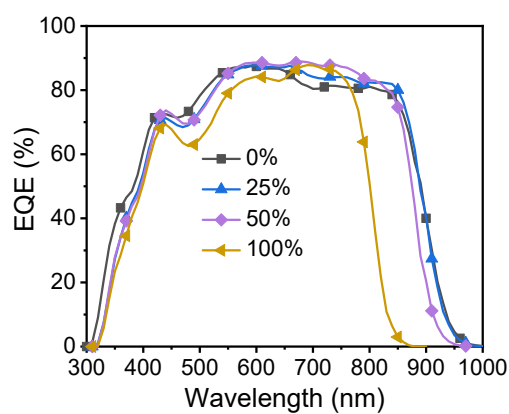
Figure S5. EQE spectra of ternary blend devices with different ratios of IT-4F.
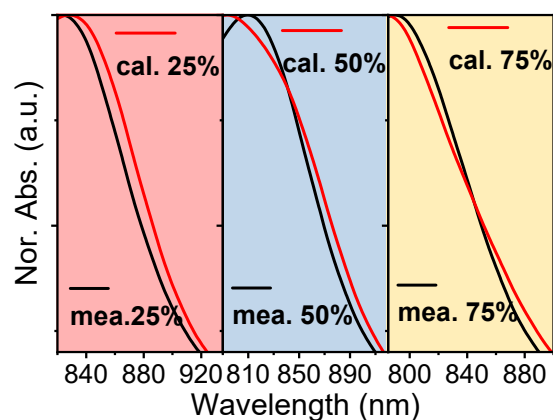
Figure S6. "Reconstructed" (referred as "cal." here) versus measured normalized UV-vis absorption spectra of mixed films (BTP-eC9 and BTP-S2).
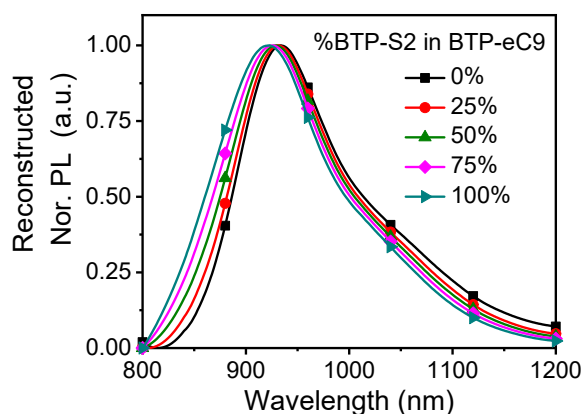
Figure S7. Reconstructed PL spectra of BTP-eC9:BTP-S2 blend films.
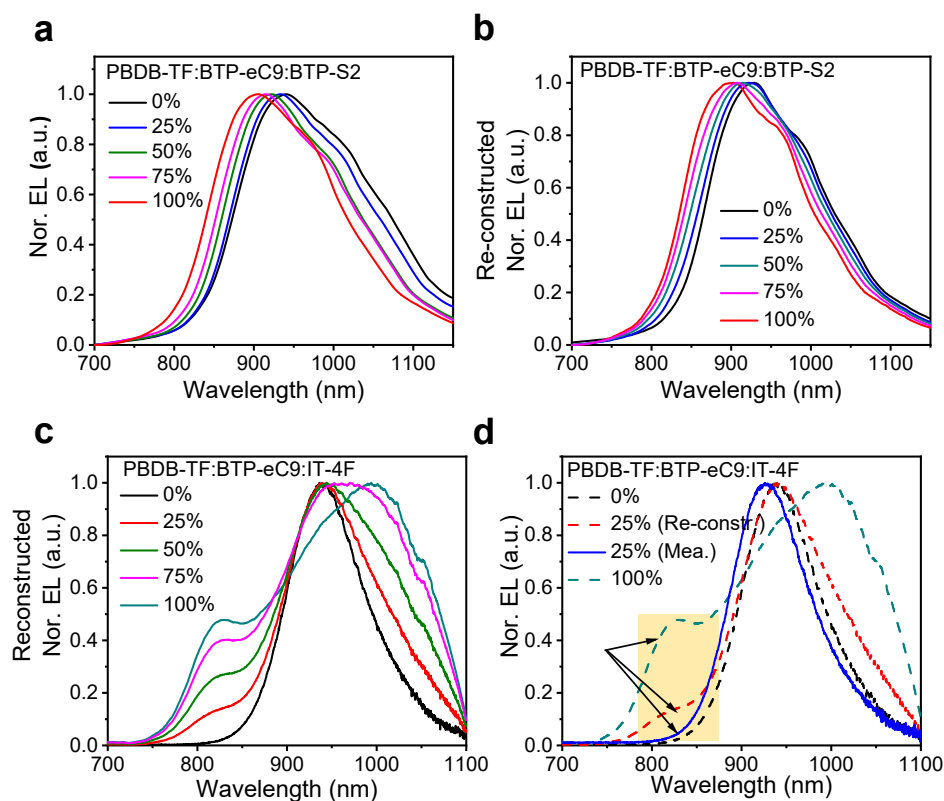
Figure S8. a) Experimental EL and b) reconstructed EL spectra of ternary devices with different ratios of BTP-S2; c) reconstructed EL spectra of ternary devices and d) experimental EL with different ratios of IT-4F.
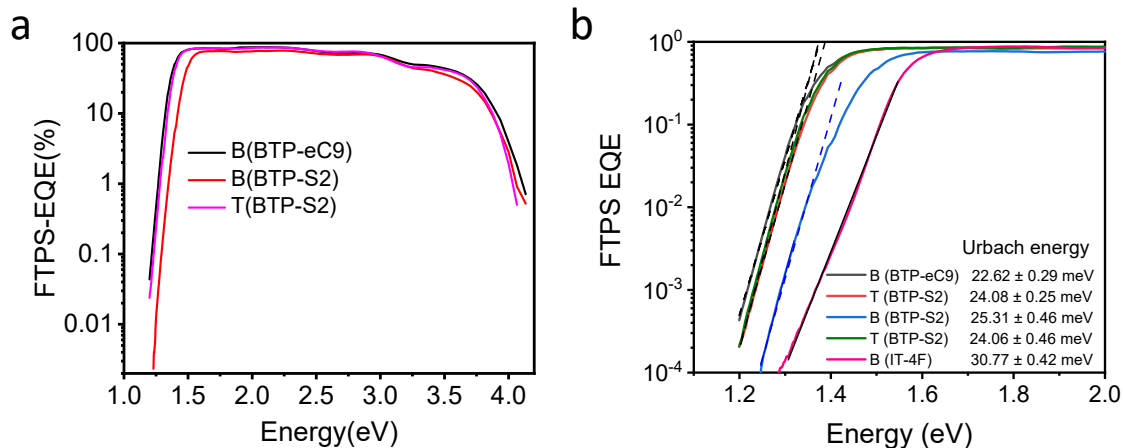
Figure S9. a) FTPS-EQE for PBDB-TF:BTP-eC9, PBDB-TF:BTP-eC9:BTP-S2 and PBDB-TF:BTP-S2 based OPVs; **b)** Urbach energy fitting with FTPS-EQE.
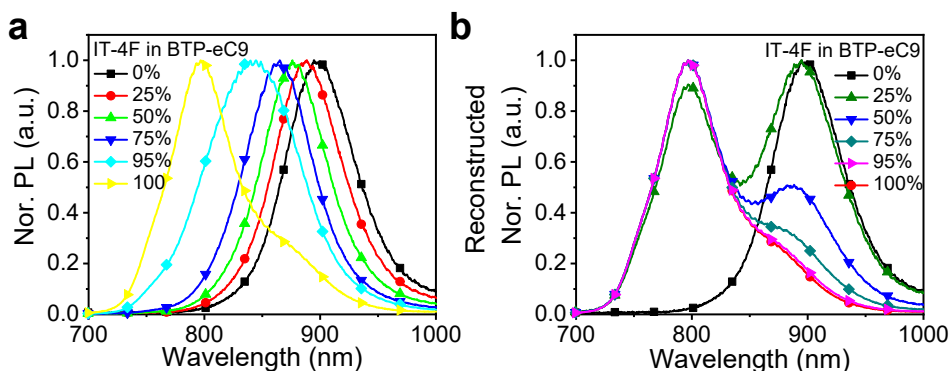
Figure S10. Reconstructed PL and experimental PL spectra of BTP-eC9:IT-4F blend films.
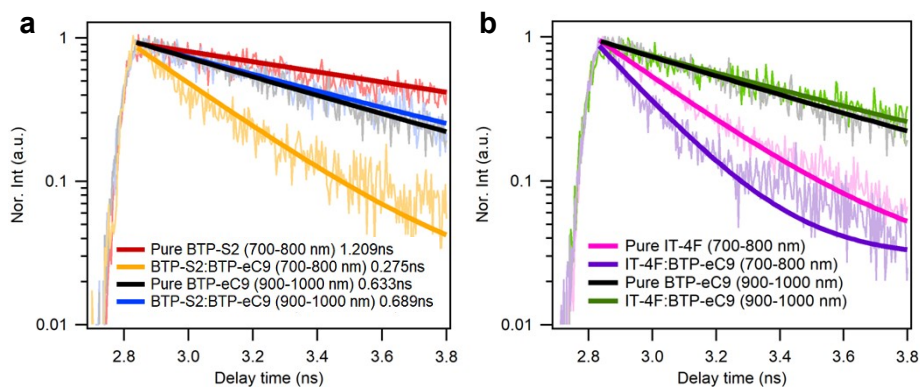
Figure S11. a) Time-resolved photoluminescence spectroscopy of BTP-eC9, BTP-S2, and BTP-eC9:BTP-S2 (0.75:0.25) blend film. b) Time-resolved photoluminescence spectroscopy of BTP-eC9, IT-4F, and BTP-eC9:IT-4F (0.75:0.25) blend film.
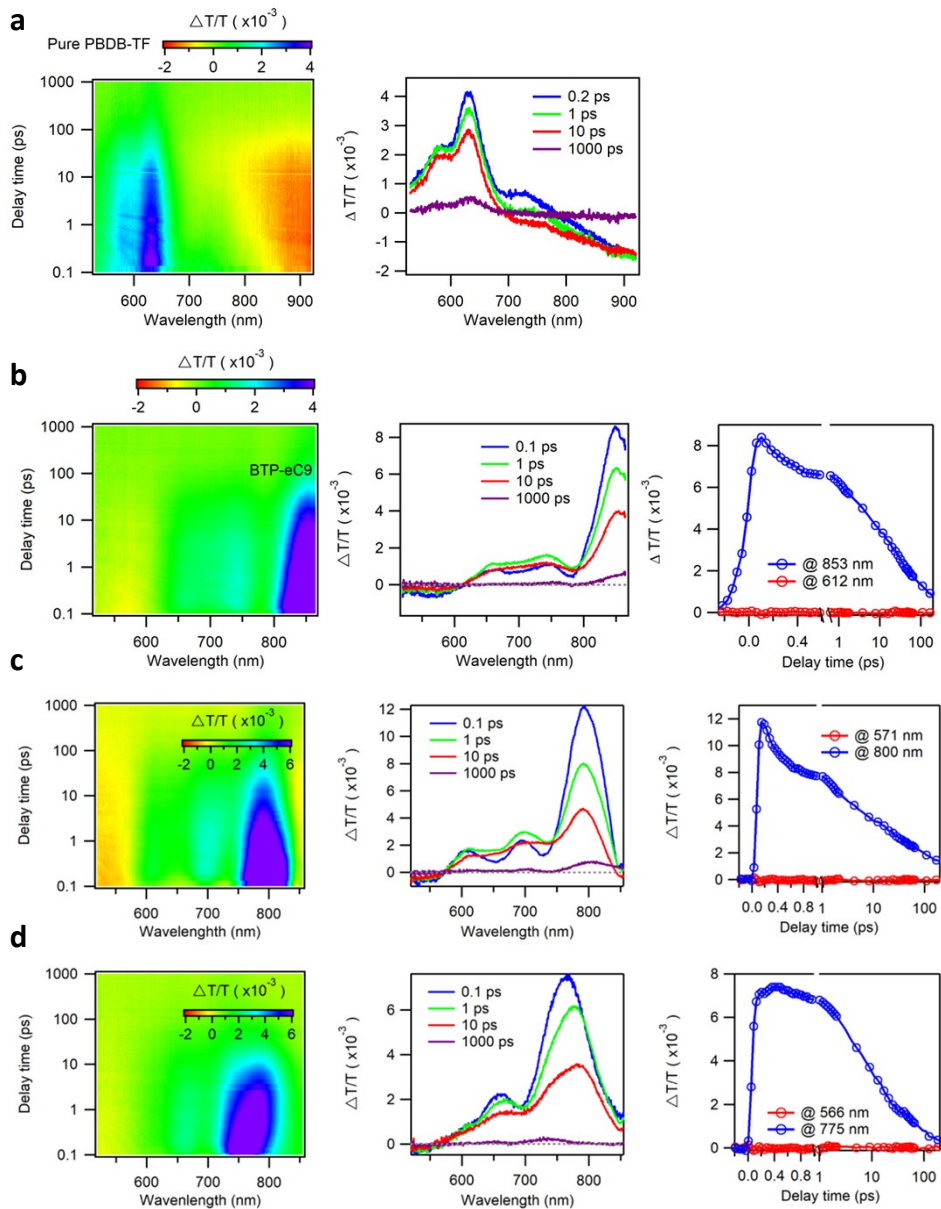
Figure S12. 2D color plots of TA spectra, TA kinetics curves at decay time of 0.1, 1, 10, 1000 ps and selective decay of featured GSB of pure a) PBDB-TF, b) BTP-eC9, c) BTP-S2, d) IT-4F.
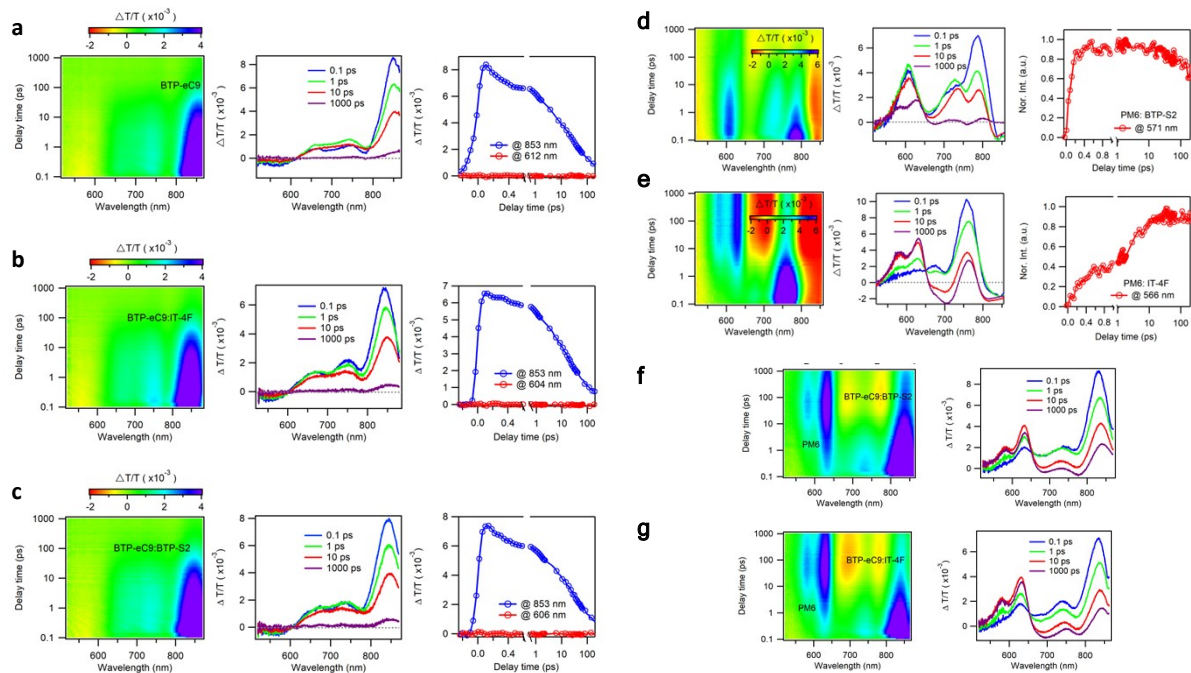
Figure S13. 2D color plots of TA spectra, TA kinetics curves at decay time of 0.1, 1, 10, 1000 ps and selective decay of featured GSB of a) BTP-eC9, b) BTP-eC9:IT-4F, c) BTP-eC9:BTP-S2, d) PBDB-TF:BTP-S2, e) PBDB-TF:IT-4F, f) PBDB-TF:BTP-eC9:BTP-S2, g) BTP-eC9:IT-4F at indicated delay times under 750 nm excitation with a fluence below 10 µJ/cm².
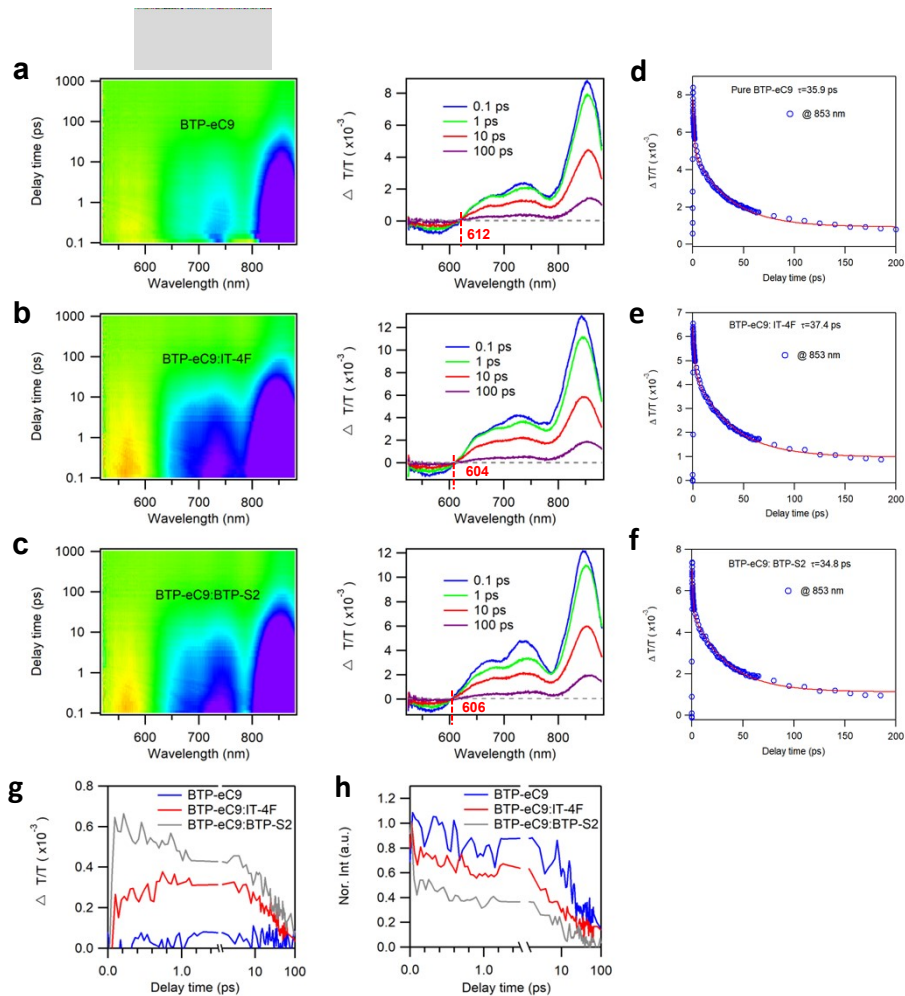
Figure S14. 2D color plots of TA spectra, TA kinetics curves at decay time of 0.1, 1, 10, 1000 ps and of a) BTP-eC9, b) BTP-eC9:IT-4F, c) BTP-eC9:BTP-S2 at indicated delay times under 925 nm excitation with a fluence below 10 μJ/cm². GSB lifetime of d) BTP-eC9, e) BTP-eC9:IT-4F, f) BTP-eC9:BTP-S2. Selective decay of g) featured GSB at 617 nm and h) excited state absorption at 598 nm.
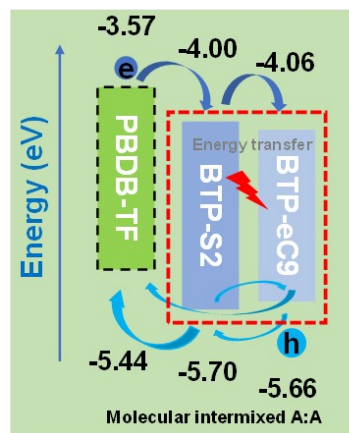
Figure S15. Schematic diagram of energy levels of each layer in device and the possible charge transfer or energy transfer dynamics.
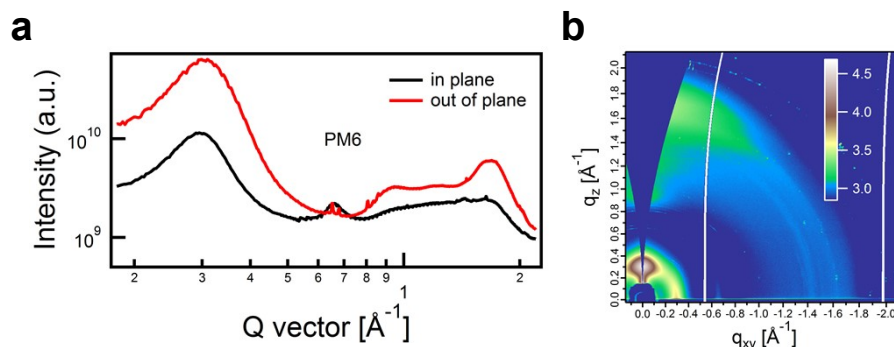
Figure S16. a) 1D intensity profiles and b) 2D GIWAX image of pure PBDB-TF film.
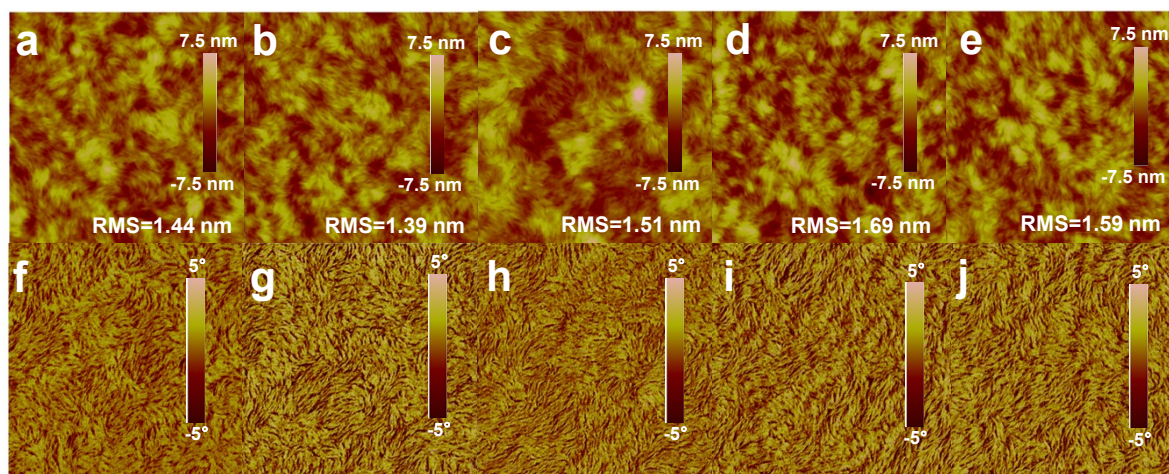
Figure S17. (a-e) AFM height images of PBDB-TF:BTP-eC9, PBDB-TF:BTP-eC9:IT-4F(25%), PBDB-TF:IT-4F, PBDB-TF:BTP-eC9:BTP-S2(25%) and PBDB-TF:BTP-S2, respectively. (f-j) Corresponding AFM phase images.
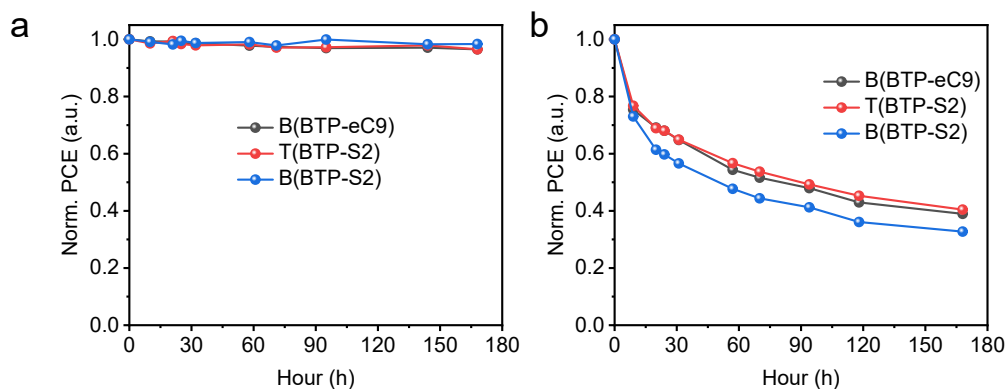
Figure S18 (a) Stability of devices stored in glove box filled with nitrogen; (b) Stability of encapsulated devices under illumination in air atmosphere.
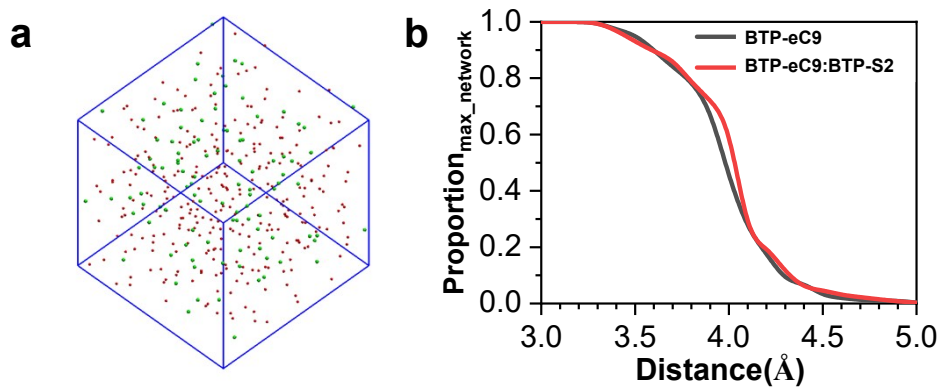
Figure S19. (a) Molecule distribution from MD simulation. The red ball represents the BTP-eC9, and the green ball for BTP-S2. (b) Proportion of the number of molecules in the largest connection network over the total number of molecules in the film, as a function of the intermolecular distance (measured as the nearest distance between heavy atoms) for the pristine BTP-eC9 film and the 25wt% BTP-S2:BTP-eC9 blending film.

Supplementary Tables

Table S1. Device parameters of recent ternary blend organic solar cell based on non-fullerene systems.

Materials	Voc (V)	Jsc (mA/cm⁻²)	FF (%)	PCE (%)	Certified PCE (%)	Reference
PBQx-TF:eC9-2Cl:F-BTA3	0.879	26.7	80.9	19.0	18.7	[11]
PBDB-TF:HDO-4Cl:eC9	0.866	27.06	80.51	18.86	18.3	[12]
PBDB-TF:BTP-eC9:L8-BO-F	0.853	27.35	80.0	18.66	18.2	[13]
PBDB-TF:BTP-eC9:BTP-F	0.858	26.99	79.7	18.45	18.0	[14]
PB2F:PBDB-TF:BTP-eC9	0.860	26.6	79.9	18.3	18.2	[15]
PBDB-TF:BO-4Cl:BTP-S2	0.861	27.14	78.04	18.16	17.8	[16]
PBDB-TF:BPR-SCl:BTPeC9	0.856	27.13	77.6	18.02	-	[17]
PBDB-TF:Y6:AQx-3	0.870	26.82	77.2	18.01	-	[18]
PBDB-TF:Y6:Y6-1O	0.900	25.87	76.92	17.91	-	[19]
PBDB-TF:PM7-Si:BTP-eC9	0.864	26.35	77.6	17.7	-	[20]
PBDB-TF:Y6:C8-DTC	0.873	26.5	75.61	17.52	-	[21]
PBDB-TF:Y6:ITCPTC	0.861	25.67	78.8	17.42	-	[22]
PBDB-TF:BTP-4F-12:MEIC	0.863	25.4	79.2	17.4	-	[23]
PBDB-TF:DRTB-T-C4:Y6	0.85	24.79	81.3	17.13	-	[24]
PBDB-TF:Y6:DRTB-T-Cl	0.854	24.68	80.88	17.05	-	[25]
PBDB-TF:Y6:BTP-M	0.875	26.56	73.46	17.03	-	[26]
PBDB-TF:SM1:Y6	0.831	25.7	77.5	16.55	-	[27]

Table S2. Summary energy loss data for binary and ternary organic solar cells.

Device	E^{PV}_g/q (V)[a]	V_{OC} (V)	Vloss (V)	V^{SQ}_{oc} (V)	V^{rad}_{oc} (V)	$\Delta V1$ (V)	$\Delta V2$ (V)	$\Delta V3$ (V)	EQE_{EL} (%)	Exp. $V^{non-rad}_{oc}$ (V)
B(BTP-eC9)	1.3764	0.845	0.5314	1.1144	1.0726	0.2620	0.0418	0.2276	0.00602	0.2517
B(IT-4F)	1.5610	0.854	0.7070	1.2859	1.2063	0.2750	0.0796	0.3524	0.000077	0.3645
T(IT-4F)	1.3868	0.852	0.5328	1.1227	1.0833	0.2641	0.0394	0.2293	0.00584	0.2525
B(BTP-S2)	1.4832	0.951	0.5322	1.2123	1.1436	0.2709	0.0687	0.1926	0.03418	0.2067
T(BTP-S2)	1.3942	0.873	0.5212	1.1308	1.0864	0.2634	0.0444	0.2134	0.01104	0.2360

$$E^{PV}_g = \frac{\int_b^a E_g P(E_g)dE_g}{\int_b^a P(E_g)dE_g}$$

[a] The bandgap in voltage loss section is means photovoltaic bandgap ($E^{PV}_g = \frac{\int_b^a E_g P(E_g)dE_g}{\int_b^a P(E_g)dE_g}$), which is extracted from EQE

Table S3. The lifetime constants fitting from transient absorption spectra.

Device	A1	$\tau 1$(ps)	A2	$\tau 2$(ps)
B(BTP-eC9)	51.6%	0.228 ± 0.02	48.4%	8.94 ± 0.89
T(IT-4F)	53.4%	0.284 ± 0.03	46.6%	7.31 ± 0.73
T(BTP-S2)	56.8%	0.188 ± 0.02	43.2%	7.41 ± 0.74

Table S4. Diffusion mediated HTE (η_2) of different BHJ films.

Samples	τ_R (ps)	τ_{DHT} (ps)	η_2 (%)
BTP-eC9	35.9	/	/
BTP-eC9:IT-4F	37.4	/	/
BTP-eC9:BTP-S2	34.8	/	/
B(BTP-eC9)	/	8.9	80.1
T(IT-4F)	/	7.3	83.7
T(BTP-S2)	/	7.4	82.5

Table S5. HTE (η_{HT}) of different BHJ films

Samples	α	β	η_2 (%)	η_{HT} (%)
B(BTP-eC9)	0.516	0.484	80.1	90.3

T(IT-4F)	0.534	0.466	83.7	92.4
T(BTP-S2)	0.568	0.432	82.5	92.4

Table S6. Summarized data derived from GIWAX.

pi-pi	Location	Intensity	d-spacing/nm	CL/nm
BTP-eC9	1.74	2.87E+08	0.36	2.19
BTP-S2	1.76	4.83E+09	0.36	2.27
IT-4F	1.77	2.33E+09	0.36	2.23
BTP-eC9: BTP-S2	1.76	9.39E+08	0.36	2.14
BTP-eC9:IT-4F	1.76	2.86E+09	0.36	2.15
B(BTP-eC9)	1.76	4.83E+09	0.36	2.41
B(BTP-S2)	1.79	5.83E+09	0.35	2.56
B(IT-4F)	1.77	1.27E+09	0.35	2.13
T(BTP-S2)	1.76	3.70E+09	0.36	2.35
T(IT-4F)	1.75	3.61E+09	0.36	2.37

References.

1. S. Li, L. Zhan, Y. Jin, G. Zhou, T. K. Lau, R. Qin, M. Shi, C. Z. Li, H. Zhu, X. Lu, F. Zhang and H. Chen, *Adv. Mater.*, 2020, **32**, 2001160.
2. B. Hess, C. Kutzner, D. van der Spoel and E. Lindahl, *J. Chem. Theory Comput.*, 2008, **4**, 435-447.
3. J. Wang, R. M. Wolf, J. W. Caldwell, P. A. Kollman and D. A. Case, *J. Comput. Chem.*, 2004, **25**, 1157-1174.
4. C. I. Bayly, P. Cieplak, W. Cornell and P. A. Kollman, *J. Phys. Chem.*, 1993, **97**, 10269-10280.
5. L. Zhu, J. Zhang, Y. Guo, C. Yang, Y. Yi and Z. Wei, *Angew. Chem. Int. Ed.*, 2021, **60**, 15348-15353.
6. G. Bussi, D. Donadio and M. Parrinello, *J. Chem. Phys.*, 2007, **126**, 014101.
7. H. J. C. Berendsen, J. P. M. Postma, W. F. van Gunsteren, A. DiNola and J. R. Haak, *J. Chem. Phys.*, 1984, **81**, 3684-3690.
8. S. Nosé, *J. Chem. Phys.*, 1984, **81**, 511-519.
9. W. G. Hoover, *Physical Review A*, 1985, **31**, 1695-1697.
10. M. Parrinello and A. Rahman, *J. Appl. Phys.*, 1981, **52**, 7182-7190.
11. Y. Cui, Y. Xu, H. Yao, P. Bi, L. Hong, J. Zhang, Y. Zu, T. Zhang, J. Qin, J. Ren, Z. Chen, C. He, X. Hao, Z. Wei and J. Hou, *Adv. Mater.*, 2021, **33**, 2102420.

12. P. Bi, S. Zhang, Z. Chen, Y. Xu, Y. Cui, T. Zhang, J. Ren, J. Qin, L. Hong, X. Hao and J. Hou, *Joule*, 2021, DOI: 10.1016/j.joule.2021.06.020.
13. Y. Cai, Y. Li, R. Wang, H. Wu, Z. Chen, J. Zhang, Z. Ma, X. Hao, Y. Zhao, C. Zhang, F. Huang and Y. Sun, *Adv. Mater.*, 2021, DOI: 10.1002/adma.202101733, 2101733.
14. Y. Li, Y. Cai, Y. Xie, J. Song, H. Wu, Z. Tang, J. Zhang, F. Huang and Y. Sun, *Energy Environ. Sci.*, 2021, DOI: 10.1039/d1ee01864g.
15. T. Zhang, C. An, P. Bi, Q. Lv, J. Qin, L. Hong, Y. Cui, S. Zhang and J. Hou, *Adv. Energy Mater.*, 2021, **11**.
16. L. Zhan, S. Li, X. Xia, Y. Li, X. Lu, L. Zuo, M. Shi and H. Chen, *Adv. Mater.*, 2021, **33**, 2007231.
17. X. Chen, D. Wang, Z. Wang, Y. Li, H. Zhu, X. Lu, W. Chen, H. Qiu and Q. Zhang, *Chem. Eng. J.*, 2021, **424**.
18. F. Liu, L. Zhou, W. Liu, Z. Zhou, Q. Yue, W. Zheng, R. Sun, W. Liu, S. Xu, H. Fan, L. Feng, Y. Yi, W. Zhang and X. Zhu, *Adv. Mater.*, 2021, **33**, 2100830.
19. X. Ma, A. Zeng, J. Gao, Z. Hu, C. Xu, J. H. Son, S. Y. Jeong, C. Zhang, M. Li, K. Wang, H. Yan, Z. Ma, Y. Wang, H. Y. Woo and F. Zhang, *Natl Sci Rev*, 2021, **8**, nwaa305.
20. W. Peng, Y. Lin, S. Y. Jeong, Y. Firdaus, Z. Genene, A. Nikitaras, L. Tsetseris, H. Y. Woo, W. Zhu, T. D. Anthopoulos and E. Wang, *Chem. Mater.*, 2021, **33**, 7254-7262.
21. Q. Ma, Z. Jia, L. Meng, J. Zhang, H. Zhang, W. Huang, J. Yuan, F. Gao, Y. Wan, Z. Zhang and Y. Li, *Nano Energy*, 2020, **78**.
22. R. J. Ma, T. Liu, Z. H. Luo, K. Gao, K. Chen, G. Y. Zhang, W. Gao, Y. Q. Xiao, T. K. Lau, Q. P. Fan, Y. Z. Chen, L. K. Ma, H. L. Sun, G. L. Cai, T. Yang, X. H. Lu, E. G. Wang, C. L. Yang, A. K. Y. Jen and H. Yan, *ACS Energy Lett.*, 2020, **5**, 2711-2720.
23. X. Ma, J. Wang, J. Gao, Z. Hu, C. Xu, X. Zhang and F. Zhang, *Adv. Energy Mater.*, 2020, DOI: 10.1002/aenm.202001404.
24. D. Li, L. Zhu, X. Liu, W. Xiao, J. Yang, R. Ma, L. Ding, F. Liu, C. Duan, M. Fahlman and Q. Bao, *Adv. Mater.*, **n/a**, 2002344.
25. Y. Zeng, D. Li, Z. Xiao, H. Wu, Z. Chen, T. Hao, S. Xiong, Z. Ma, H. Zhu, L. Ding and Q. Bao, *Adv. Energy Mater.*, 2021, **11**.
26. L. L. Zhan, S. X. Li, T. K. Lau, Y. Cui, X. H. Lu, M. M. Shi, C. Z. Li, H. Y. Li, J. H. Hou and H. Z. Chen, *Energy Environ. Sci.*, 2020, **13**, 635-645.
27. T. Yan, J. Ge, T. Lei, W. Zhang, W. Song, B. Fanady, D. Zhang, S. Chen, R. Peng and Z. Ge, *J. Mater. Chem. A*, 2019, **7**, 25894-25899.